

# CFD Simulations of Gas–Liquid Multiscale Flow Characteristics in an Aluminum Electrolysis Cell with Population Balance Model: Effect of Anode Slot Configuration

SHUIQING ZHAN,<sup>1</sup> YUJIE HUANG,<sup>1</sup> ZHENTAO WANG,<sup>1</sup>  
CHANGFENG LI,<sup>1</sup> JIANHONG YANG,<sup>2</sup> and JUNFENG WANG<sup>1,3</sup>

1.—School of Energy and Power Engineering, Jiangsu University, Zhenjiang 212013, People's Republic of China. 2.—School of Material Science and Engineering, Jiangsu University, Zhenjiang 212013, People's Republic of China. 3.—e-mail: wangjunfeng@ujs.edu.cn

Numerical simulations of the effects of different anode slot configurations on the gas–liquid multiscale flow characteristics in an aluminum electrolysis cell have been conducted based on a recently developed mathematical model. The results clearly showed that use of anode slots can significantly promote the bubble evacuation behavior and thus affect the overall flow pattern. Both the gas volume fraction and bubble size decreased obviously when transversal or especially longitudinal slots were used. Moreover, the greater the number of both kinds of slot, the lower the mentioned parameters. With increasing anode slot width, the gas volume fraction decreased slightly while there was almost no effect on the bubble size distribution (BSD). Reducing the anode slot height caused a higher gas volume fraction. Both the overall gas volume fraction and BSD in industrial-scale cells are apparently influenced by two large circulation vortices caused by electromagnetic forces (EMFs).

## INTRODUCTION

The only industrial route for producing aluminum from alumina is the Hall–Héroult process, in which anodic bubbles are mainly generated under the bottom surface of the anodes due to electrochemical reactions. These bubbles then move horizontally and upward to the top surface of the electrolyte, consequently creating well-known macroscopic two-phase gas–liquid flows under the combined effects of gas-driven and electromagnetic forces (EMFs). Meanwhile, typical mesoscale interactions, mainly including bubble nucleation, growth, coalescence, and breakup, are enhanced due to the limitation of the large-scale horizontal anodes used in industrial cells, eventually resulting in a continuous gas bubble layer with different sized bubbles. These macroscopic/mesoscale physical phenomenon strongly influence the overall performance of the cell. On the one hand, the macroscopic gas-induced electrolyte flow plays an important and positive role in the overall cell thermal balance as well as the dissolution, dispersion, and transport characteristics of the alumina particles. On the other hand, the

dynamic evolution of the mesoscale bubble layer has a negative impact on the conductivity of the electrolyte and the contact oxidation process between the bubbles and molten aluminum, thus inevitably resulting in high cell voltage drop and low current efficiency.<sup>1</sup>

Over the past two decades, although significant achievements have been made to fully utilize the advantages of the macroscopic electrolyte flow hydrodynamics for the design, operation, and scale-up of industrial cells, some key problems emphasized above have not been completely solved due to the complex and unknown behavior of the bubbles. However, development of anodes and cathodes with new structures has attracted great attention, and the widely used slotted anode configuration has proven highly effective for solving these problems, mainly because the slots in the anode enable better evacuation of gas bubbles from the bottom regions of the anode.<sup>2,3</sup> However, this design also suffers from some negative effects, such as shortened anode lifecycle, carbon dross rise, and increased iron content in the molten aluminum.<sup>3,4</sup> The main reason may be that the design and

optimum operation of these slotted anodes have largely been empirical. Therefore, further research and exploration of anode slot configurations and their fundamental effects on the two-phase gas–liquid flow characteristics will be beneficial for efficient design and scale-up of such electrolysis reactors.

Due to the high temperature, corrosive environment, and low transparency in the bath, it is extremely difficult to conduct direct measurements in industrial cells. Therefore, various experimental approaches, including large-scale low-temperature air–water,<sup>5,6</sup> and electrolytic experiments,<sup>7,8</sup> and small-scale high-temperature electrolytic experiments<sup>9,10</sup> as well as numerical methods<sup>11–14</sup> have been extensively proposed in the open literature. However, neither low-temperature air–water nor electrolytic experiments are perfect, due to their restrictions in terms of experimental conditions, as the mesoscale bubble generation mechanism differs from the actual electrochemical reaction. Meanwhile, due to anode scale limitations, the macroscopic/mesoscale gas–liquid flow characteristics in small-scale high-temperature electrolytic systems are rather different from the features of practical electrolytic systems. As detailed in recent research,<sup>15</sup> although these experimental approaches provide some experience, they have been restricted to some extent for industrial-scale applications due to their specific conditions. Therefore, further analysis and investigation should be carried out to compensate for these shortcomings.

With the significant development of numerical calculation technology, the well-known Eulerian–Eulerian two-fluid model in computational fluid dynamics (CFD) has been widely applied to simulate two-phase gas–liquid flows in large-scale industrial cells. The main aim of this method is to apply CFD to predict information about the bulk flow characteristics, suitable for the design and scale-up of cells.<sup>11–15</sup> CFD modeling of the effects of anode slots can help to choose the most promising configurations before testing in industrial cells. Based on application experience of such designs, the slots in the anodes can be either longitudinal or transversal. Yang et al.<sup>16</sup> simulated the effects of the slot width and height on the electrolyte flow under various cell operation conditions. Severo et al.<sup>17</sup> proposed a CFD method to investigate the effects of different slotted anodes on the gas-induced electrolyte flow. Yang et al.<sup>18</sup> proposed CFD simulations of the effects of longitudinal, transversal, and vertical slots in anodes on the gas evacuation process in detail. Our team also investigated the effects of anodes with longitudinal and transversal slot configurations on the distributions of the electrolyte flow, gas volume fraction, and alumina concentration based on the Eulerian–Eulerian two-fluid approach.<sup>19</sup> Although such CFD approaches have achieved some success in the theoretical analysis and engineering design of slotted anodes, the fundamental physical

mechanisms occurring between the different phases are still not deeply and fully understood. The most important outstanding issue is the development of an accurate mathematical model to describe such gas–liquid flows perfectly. Encouragingly, our group<sup>20</sup> made important discoveries on reasonable and systematic closures of the Eulerian–Eulerian gas–liquid two-fluid approach based on innovative experiments carried out by Cooksey et al.,<sup>6</sup> particularly regarding the strict prediction performance of different interphase forces and turbulence models. Other key issues include modeling the mesoscale bubble behavior and ensuring accurate coupling between the different scales and phases, which are also the main drawbacks of previous CFD models. Again, we innovatively proposed a coupled computational fluid dynamics–population balance model (CFD–PBM) that considers appropriate bubble coalescence and breakup mechanisms, to explore the well-accepted mesoscale bubble distribution characteristics and overall macroscopic two-phase flows.<sup>15</sup> However, systematic and detailed investigations of the effects of different anode slot configurations on the gas–liquid multiscale flow characteristics inside aluminum electrolysis cells are still required.

The primary objective of the work presented herein is to extend our previous research<sup>15</sup> by examining the effects of different anode slot configurations on the gas–liquid multiscale flow characteristics in terms of electrolyte flow, gas volume fraction, and bubble size distribution (BSD) with detailed discussion employing CFD–PBM simulations. Furthermore, the EMFs in a 300-kA aluminum electrolysis cell were considered to improve understanding of some of the design and scale-up considerations for industrial-scale cells.

## MATHEMATICAL MODEL

### Model Description

In the framework of the macroscopic Eulerian–Eulerian approach, the continuity and momentum conservation equations were solved to investigate the overall gas–liquid two-phase flows. The dispersed standard  $k$ – $\epsilon$  model and the standard wall function were used to solve the averaged turbulent motion equations. Mesoscale population balance equations (PBEs) were built to analyze bubble groups with different numbers, sizes, and spatial distributions, considering bubble coalescence only induced by turbulence eddies and bubble breakup only due to isotropic turbulence. Since the CFD–PBM coupled model has been described and well validated carefully in earlier work, we refer to previous literature<sup>15</sup> for the detailed equations.

### Simulation Conditions

In the present study, two kinds of computational geometrical model, including a single-anode model and a 300-kA aluminum electrolysis cell model, are

considered. For more detailed information about the main geometrical parameters of the 300-kA cell, such as the anode dimensions, anode–cathode distance (ACD), interanode channel, side channel, end channel, and center channel, see our previous study.<sup>19</sup> The basic single-anode model (also considered as a submodel) is a simplified model of the three-anode model applied by Cooksey et al.,<sup>6</sup> with similar anode dimensions and other geometrical structures. This single-anode model is used to study the base effects of the different anode slot configurations, such as the slot number (one or two), direction (longitudinal or transversal), width, height, etc. For the base simulation, the width and height of both the longitudinal and transversal slots were taken as 20 mm and 160 mm, respectively. Moreover, the entire bottom surface of the anode was divided uniformly by one or two slots, as shown in Fig. 1. Furthermore, 300-kA cell models with one longitudinal or transversal slot in each anode were used as an application and scale-up case to simulate the effects of EMFs on the overall gas–liquid multiscale flow characteristics. As stated in our previous study,<sup>15</sup> all the simulation models in this work were also created and meshed with hexahedral cells using the Fluent preprocessor Gambit. Moreover, local grid refinements was applied in the ACD regions, interanode channels, and slot channels.

The bottom surface of the anode was treated using a mass-flow inlet boundary condition with average equivalent inlet gas volume fraction of 0.5. The mass flow rates of anode gas generation were obtained using Faraday’s laws of electrolysis. For the traditional anode (without slots), a degassing boundary condition was applied only the top surface of the electrolyte, representing an outlet for the dispersed gas phase. However, for the slotted anode designs, a degassing boundary condition was also set at the slot surface. In addition, no-slip and free-slip wall boundary conditions were applied for the continuous electrolyte and dispersed gas bubbles at the walls, respectively. The detailed simulation conditions for the PBEs with the class method (CM) have been well described in previous work.<sup>15</sup>

All the CFD–PBM simulations were conducted using the commercial CFD package Fluent 16.0 with the double-precision model. The phase-coupled SIMPLE algorithm was used to couple the pressure and momentum equations. Second-order upwind discretization schemes were chosen for all equations. The underrelaxation factors for pressure, momentum, volume fraction, and PBEs used in the model were 0.2, 0.2, 0.1, and 0.05, respectively. All simulations were performed on a 2× Intel Xeon E5 2678 v3 platform with 64 GB of RAM.

## RESULTS AND DISCUSSION

As emphasized in the previous section and prior research,<sup>15,21</sup> because both the macroscopic electrolyte flows and mesoscale bubble behavior under

the bottom regions of the anode are very important, the simulation results in these regions are mainly discussed and analyzed for the different anode slot configurations. The single-anode model with a traditional anode was selected as the base case for different analyses and discussion. Note that it is not possible to consider the influence of the EMFs in the single-anode model, but it should be considered for the 300-kA aluminum electrolysis cell model.

### Effects of Anode Slot Number and Direction

Systematic comparisons of the distributions of electrolyte velocity, gas volume fraction, and bubble size on a horizontal plane at a distance of 10 mm from the bottom surface of the anode in the single-anode model for different anode slot numbers and directions are presented in Fig. 2. As describe above, the slot width and height were assumed to be 20 mm and 160 mm, respectively. Black streamlines indicate the overall flow characteristics. As seen from Fig. 2a, the electrolyte mainly flows into the ACD regions from both the side and central channels, then flows out into both sides of the interanode channels for the traditional anode. Moreover, this electrolyte flow pattern exhibits symmetrical distributions along both center lines of the anode with longitudinal and transversal directions, which is closely associated with the gas flow fields. Figure 2a shows that the gas volume fraction is higher in central regions and lower in boundary regions of the anode, which is well consistent with previous CFD simulation results proposed by others.<sup>18</sup> Besides, the gas flow exhibits a symmetric nature, similar to the electrolyte flow. It can also be observed from Fig. 2a that the larger bubbles are mainly located at the anode boundary regions near the interanode channels while the smaller bubbles are mainly found in other regions. The main reason for and a detailed explanation of this gas volume fraction and bubble size distribution were provided in our previous investigation.<sup>15</sup>

However, when the slotted anodes are considered, the simulation results change obviously, as also shown in Fig. 2. Since the slots in the anode are well known to act as additional interanode channels, gas bubbles can evacuate from these anode slots directly. Therefore, the original single anode can be equally divided into two or three so-called renewed smaller anodes for anode slot number of one or two, respectively, in the present work. Figure 2b shows that the predicted results under the bottom regions of these renewed small anodes for the anode with one longitudinal slot are very similar to those for the traditional anode. However, for the anode with two longitudinal slots, the pattern gradually changes, especially regarding the symmetrical characteristics under the bottom regions of the two small anodes near the separate interanode channels, as clearly shown in Fig. 2c. Further comparison of Fig. 2a–c reveals that the

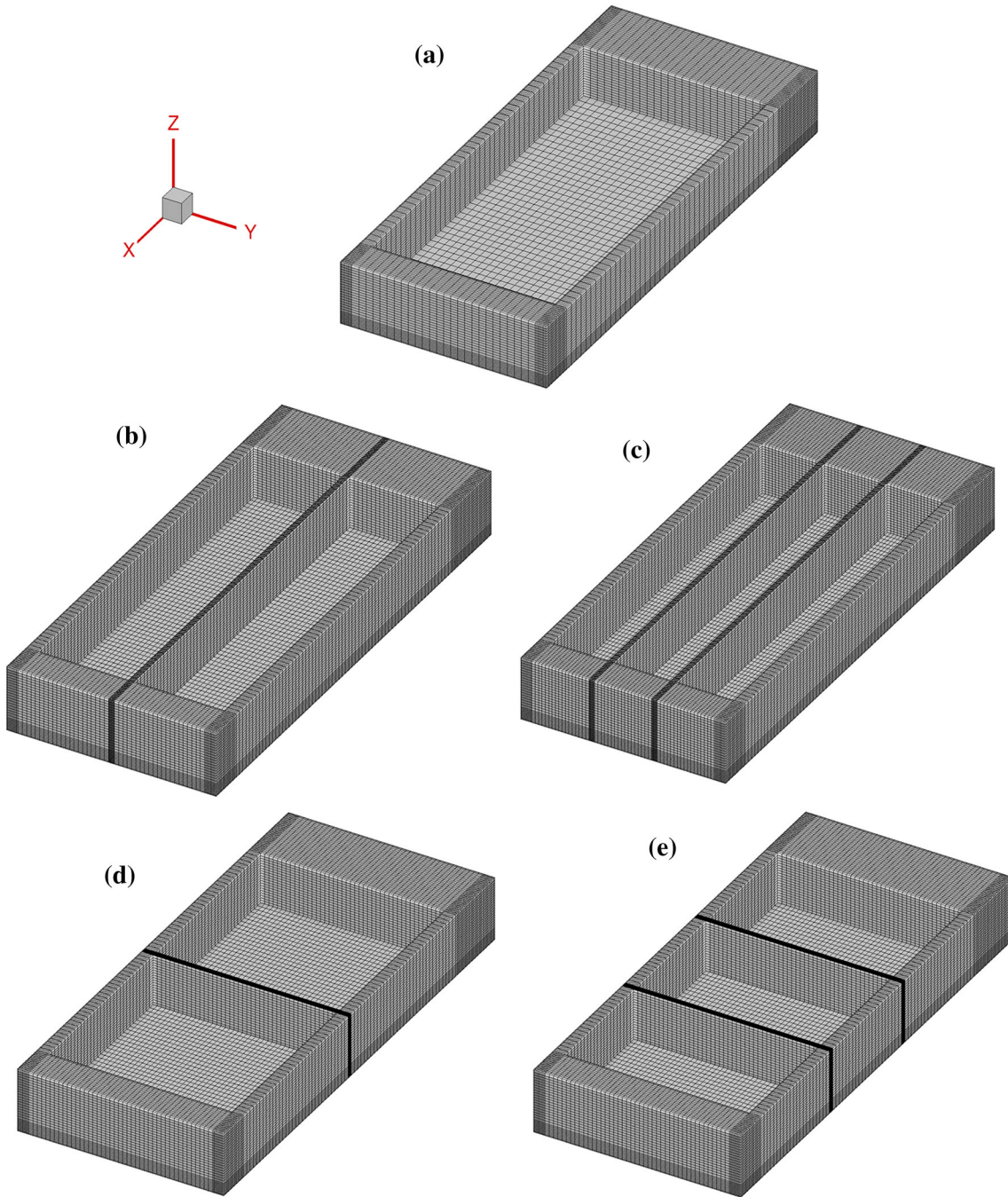


Fig. 1. Geometry and grid schemes for the single-anode model: (a) traditional anode, (b) anode with one longitudinal slot, (c) anode with two longitudinal slots, (d) anode with one transversal slot, and (e) anode with two transversal slots.

numerical values of the three parameters mentioned above decrease when longitudinal slots are used or the greater the number of slots. This occurs because such longitudinal slots can lead to rapid evacuation of gas bubbles from the bottom surface of the anode, significantly decreasing the gas volume fraction. Thus, the velocity of the electrolyte should also be decreased due to the reduced momentum exchange caused by the lower gas volume fraction. Meanwhile, since the bubble coalescence behavior plays a leading role under the bottom regions of the

anode, as confirmed in our previous investigation,<sup>15</sup> the bubble coalescence rate will inevitably decrease for the lower gas volume fractions when using longitudinal slots. Closer examination reveals that the bubble size is also more homogeneous for the anode with two longitudinal slots.

Figure 2 also clearly reveals significant differences between the results predicted for the anode with transversal slots compared with the traditional anode or the anode with longitudinal slots, which may also be closely related to the number and

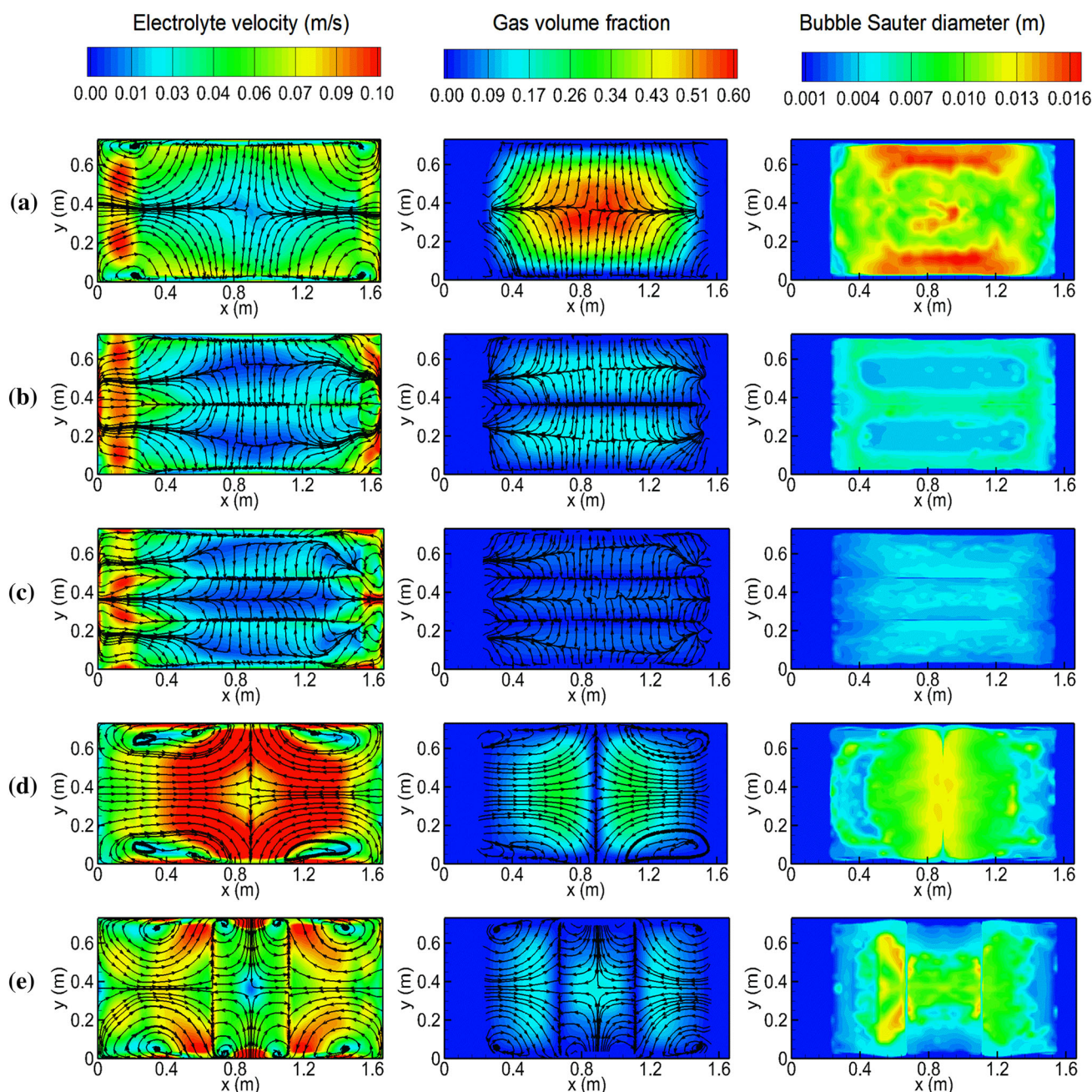


Fig. 2. Comparisons of gas–liquid flow and BSD on a horizontal plane for different anode slot numbers and directions: (a) traditional anode, (b) anode with one longitudinal slot, (c) anode with two longitudinal slots, (d) anode with one transversal slot, and (e) anode with two transversal slots.

direction of transversal slots. Generally, when one longitudinal or transversal slot is used, the traditional anode produces the highest values of gas volume fraction and bubble size, while the anode with one longitudinal slot yields the lowest values and the predicted results for the anode with one transversal slot lie somewhere in between. Similar trends are also observed when using two longitudinal or transversal slots. This can be attributed to the fact that the longitudinal and transversal slots represent approximately interanode and center channels, respectively. Due to the inherent

characteristics of the motion of the gas bubbles under the bottom regions of the horizontal anode, they prefer to travel along the anode width direction. Therefore, as expected, more gas bubbles are evacuated from the longitudinal than transversal slots, resulting in higher gas volume fractions for the anode with transversal slots than for the anode with longitudinal slots. There is an obvious increase in the electrolyte velocity for the anode with transversal slots, especially for the anode with one transversal slot, as shown in Fig. 2d. The probability of bubble coalescence will increase and more

large bubbles can be observed for the anode with transversal slots, as shown in Fig. 2c and d. Besides, similar to the effects of the number of longitudinal slots, the predicted values decrease with an increase in the number of transversal slots. As stated above, based on the general concept of reducing cell voltage drop and increasing current efficiency, industrial designs should give priority to longitudinal slots. However, in real industrial cells, use of slotted anodes can result in other problems regarding, e.g., electrolyte flow stability and the mechanical properties of the anode. Therefore, further study of this issue should be encouraged for theoretical research and practical applications. In view of the current research aim, we mainly consider the anode with one longitudinal slot as the basic single-anode model in the subsequent sections.

It is obvious from the discussion above that the longitudinal slots have significant effects on the gas–liquid flow characteristics in the ACD regions. To understand this key effect better, the predicted bubble distribution behavior in a vertical plane along the width centerline of the anode with one longitudinal slot is shown in Fig. 3. Some bubbles accumulate in the slot channels, where the gas volume fraction is obviously higher than in the side or central channels. As illustrated above, when the bubbles reach the edges of the slot, they flow into the slot with complex bubble coalescence and breakup behavior. As confirmed in previous work,<sup>15</sup> the possibility of bubble coalescence will increase with increasing local gas volume fraction while the possibility of bubble breakup increases with increase in the liquid kinetic energy dissipation rate. Careful inspection of Fig. 3c therefore reveals that the bubble size first decreases then increases as one moves up the slot, with the larger bubbles mainly appearing in the slot regions near the top surface of the electrolyte. This can be attributed to the relatively lower bubble coalescence rate and higher bubble breakup rate in the bottom regions of the slot channel and higher bubble coalescence rate and lower bubble breakup rate in the top regions of the slot.

### Effects of Anode Slot Width

Based on years of theoretical investigation and industrial practice, the anode slot width is one of the most important parameters affecting cell operating performance. Since the overall flow patterns of both phases are almost identical for different anode slot widths, comparisons of the basic flow patterns are not presented here. Therefore, only the gas volume fraction and BSD under the bottom regions of the anode for different anode slot widths of 10 mm, 15 mm, 20 mm, and 25 mm are compared in Fig. 4. The height of the longitudinal slot is kept at 160 mm for the different cases tested. Figure 4a clearly shows that the gas volume fraction decreases slightly with increasing anode slot width, especially under the

central regions of the two renewed small anodes. This is because more gas bubbles can evacuate effectively through the larger anode slot width while fewer bubbles will flow into the side or central channels. Interestingly, Fig. 4b shows that the BSD is almost the same for different anode slot widths, even though the gas volume fraction distribution differs slightly. The main reason is that the turbulent energy dissipation rate caused by gas bubble evacuation is also lower for the larger anode slot width (not shown here), thus the combined behaviors of bubble coalescence and breakup perform similarly in the different cases overall.

### Effects of Anode Slot Height

It is well known that the anode slot height will inevitably decrease due to consumption of the anode caused by the electrochemical reaction. This phenomenon is very important for deep understanding of the relationship between the evolution of the behavior of the slotted anode and its direct and indirect effects on the gas–liquid multiscale flow characteristics. The predicted results for the gas volume fraction and BSD under the bottom regions of the anode with different slot heights of 160 mm, 110 mm, 60 mm, and 0 mm (the traditional anode, as described above) are presented in Fig. 5. In addition, the predicted distributions of gas volume fraction and electrolyte velocity in the vertical middle section of the slot channel for different anode slot heights are shown in Fig. 6.

Generally, it can be seen from Fig. 5 that the gas volume fraction increases with decreasing anode slot height. When the anode slot height is decreased from 60 mm to 0 mm, the gas volume fraction increases steeply (as also illustrated in Fig. 2a). This is mainly because more bubbles can evacuate vertically from the bottom regions of the anode towards the top surface of the electrolyte when the anode slot height is larger. The larger the anode slot height, the more apparent this kind of effect. Therefore, Fig. 6a<sub>1</sub>–d<sub>1</sub> indicates that a decrease in the anode slot height will gradually hinder vertical bubble movement, hence more bubbles will be forced to flow into the side and central channels mainly via horizontal movement. Therefore, the bubble evacuation efficiency will naturally decrease, leading to higher gas volume fractions both in the slot channels and under the bottom regions of the anode. The bubble evacuation performance in the slots can cause the electrolyte to exhibit similar vertical and horizontal movements, as presented in Fig. 6a<sub>2</sub>–d<sub>2</sub>. It is observed that there exist larger local recirculation zones in both the side and central channels with larger anode slot heights, which would greatly favor local mass transfer and alumina mixing.

It is also obvious from Fig. 5 that the simulated BSDs show similar features as the anode slot height is decreased from 160 mm to 60 mm, while an entirely different BSD is predicted and larger

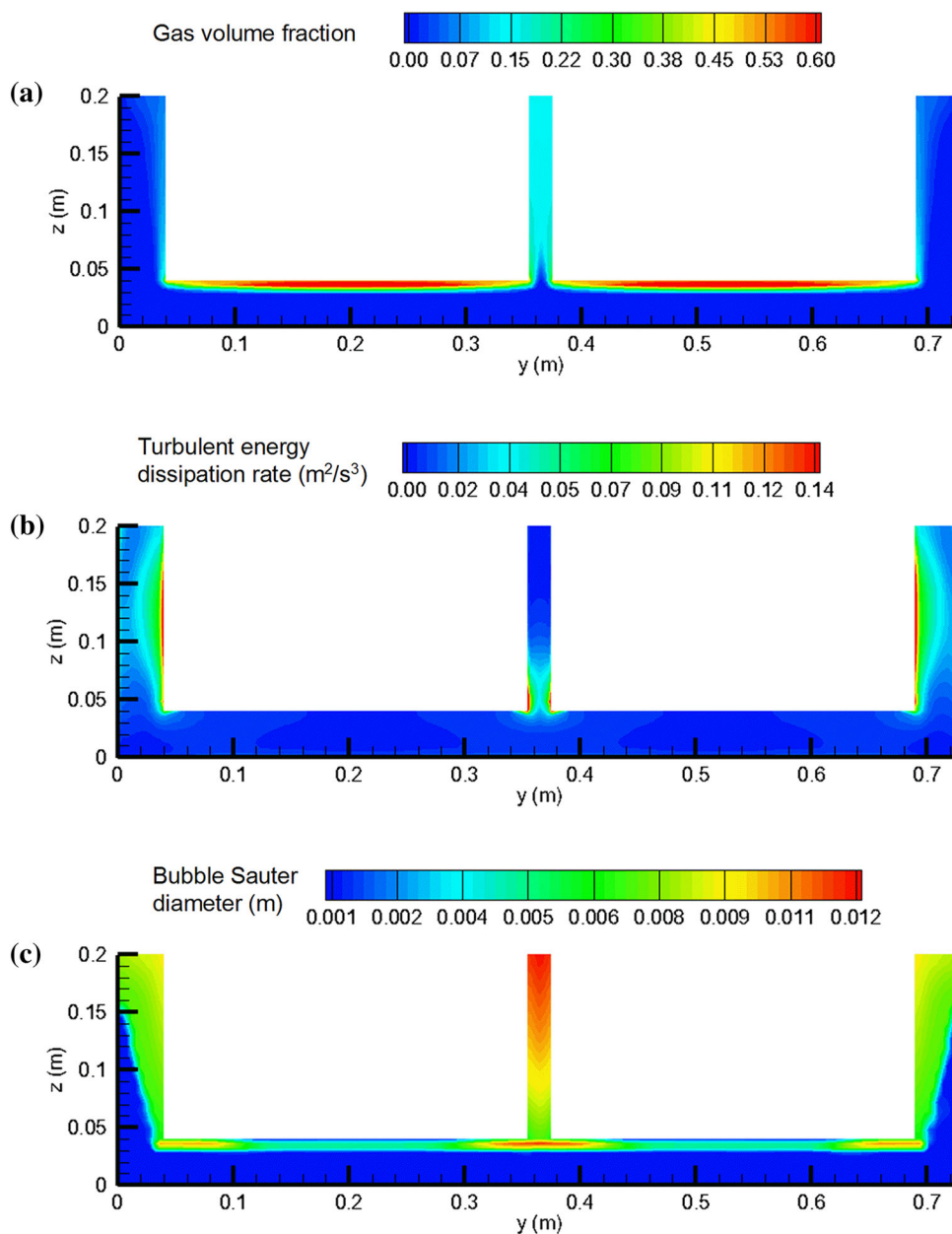


Fig. 3. Predicted distributions of (a) gas volume fraction, (b) turbulent energy dissipation rate, and (c) BSD on a vertical plane for the anode with one longitudinal slot.

bubbles can be obtained for the traditional anode. This is mainly due to the fact that the gas volume fractions are obviously different from the preceding three different cases and the combined behaviors of bubble coalescence and breakup are also similar overall. When reducing the anode slot height to about 0 mm, very high gas volume fractions can be seen (see Fig. 2a for more details), thus the bubble coalescence behavior will play a dominant role under the bottom regions of the traditional anode, as confirmed in our previous investigation.<sup>15</sup>

### Effects of Slotted Anode for 300-kA Aluminum Electrolysis Cell Coupled with EMFs

The above conclusions regarding the single-anode model without considering EMFs provide a fundamental theoretical basis for evaluating and optimizing the actual effects of different anode slot configurations for use in modern large-scale industrial cells. However, both EMFs and bubble driving forces have an important impact on the flow performance in real industrial cells. Therefore, as an extended application of the single-anode model, the

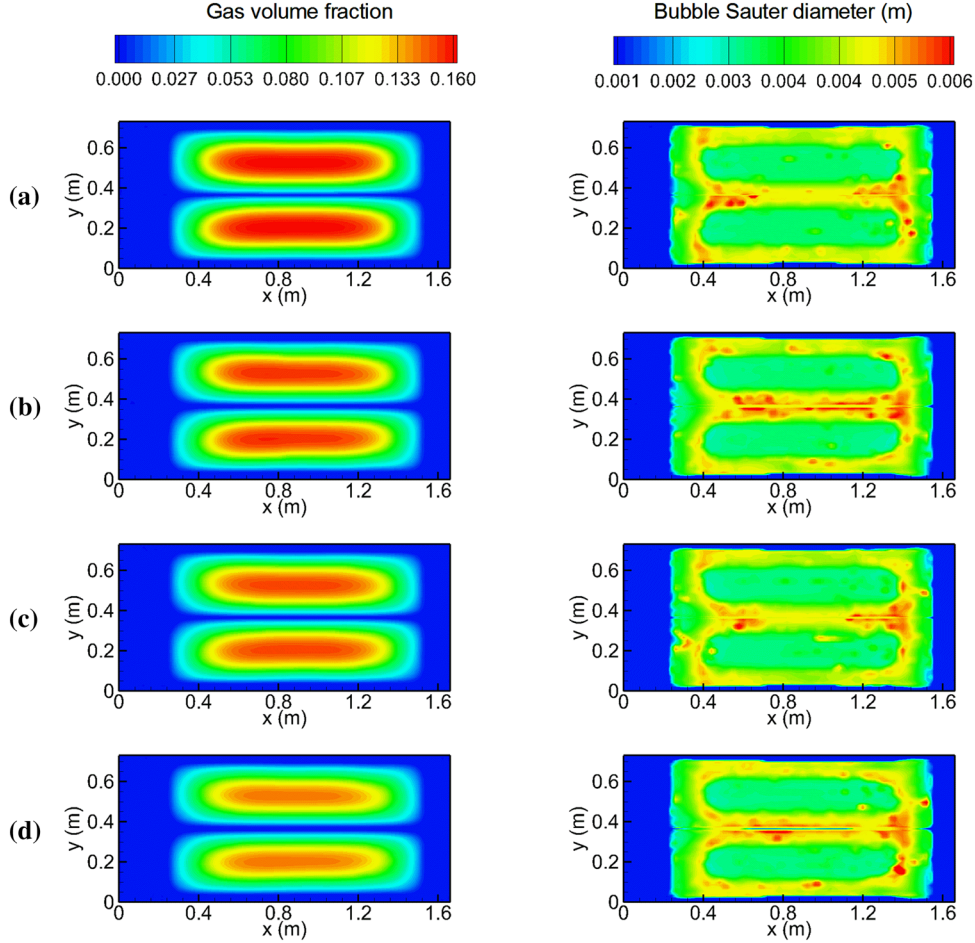


Fig. 4. Comparisons of gas volume fraction and BSD on a horizontal plane for different anode slot widths of (a) 10 mm, (b) 15 mm, (c) 20 mm, and (d) 25 mm.

CFD–PBM approach considering EMFs was proposed to further test the effects of different anode slot configurations on the gas–liquid multiscale flow characteristics in a 300-kA aluminum electrolysis cell model. To remain feasible, the present study only considers the traditional anode, and the anode with one longitudinal or transversal slot. The slot width and height are also 20 mm and 160 mm, respectively. The detailed characteristics of the EMFs obtained from ANSYS are not given in the present work. For those truly interested in them, more details can be found in our recent research.<sup>15</sup>

The predicted overall distributions of the gas–liquid two-phase flow and BSD in a horizontal plane at a distance of 10 mm from the bottom surface of the anode in the ACD regions in the 300-kA aluminum electrolysis cell considering the EMFs are shown in Fig. 7. Figure 7a<sub>1</sub>–c<sub>1</sub> clearly shows that the simulated overall electrolyte velocity distributions for the three different anode slot configurations are basically the same in terms of the flow pattern, mainly exhibiting two large, roughly circulatory vortices. However, there are also some differences between the above simulation cases, mainly in terms of a series of small local flow

circulation vortices around each traditional anode and renewed small anode and their significant impacts on the two large circulation vortices. Moreover, note that the electrolyte velocity decreases significantly for the slotted anode, particularly for the anode with one longitudinal slot. As expected, the electrolyte flow characteristics have a close relationship with the EMFs and the gas bubble evacuation behavior, as discussed above. The gas velocity distributions under the bottom regions of the anode in Fig. 7a<sub>2</sub>–c<sub>2</sub> are nearly the same as the electrolyte velocity distributions for all three cases. Moreover, the horizontal gas velocity for the traditional anode is obviously higher than that for the slotted anodes. One possible reason is that the reduced electrolyte velocity under the bottom regions of the anode can in turn slow the bubble evacuation behavior. Note that no relevant reports on the overall horizontal gas flow patterns in full industrial aluminum electrolysis cells have been reported to date.

Figure 7a<sub>3</sub>–c<sub>3</sub> clearly shows that the local gas volume fraction under the bottom region of each slotted anode is significantly lower than for the traditional anode, especially for one longitudinal



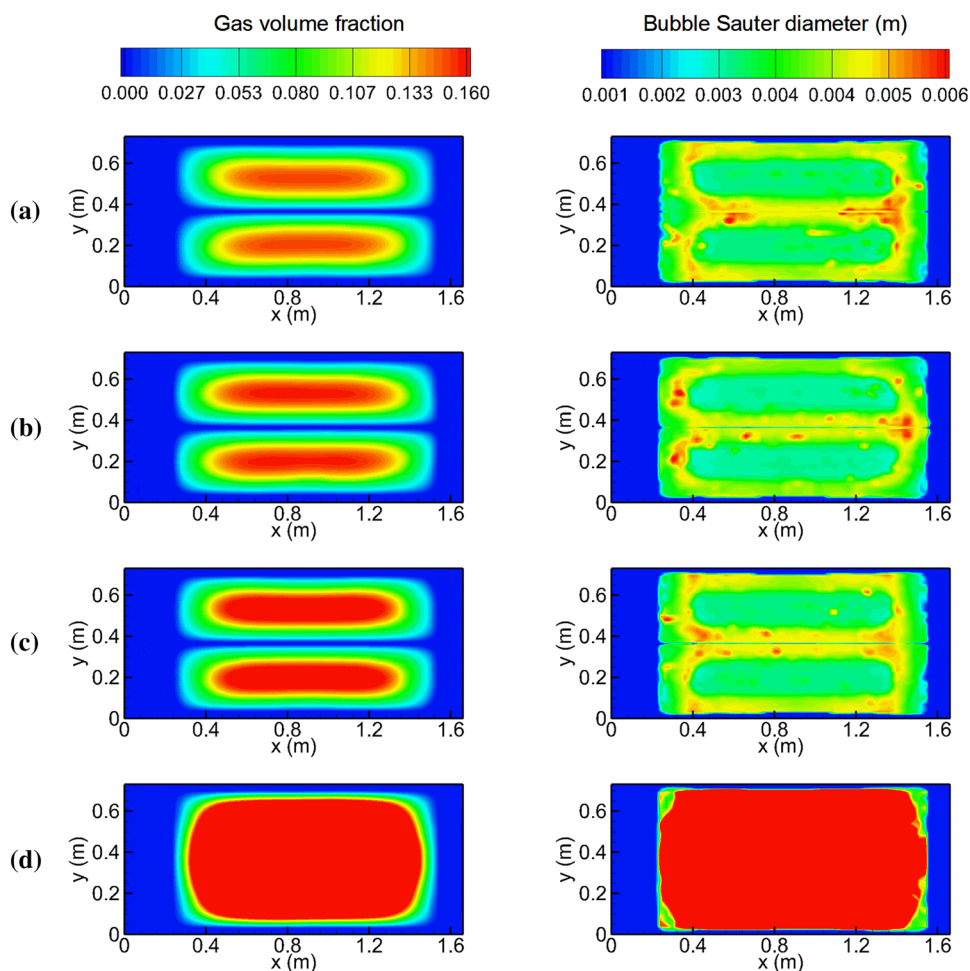


Fig. 5. Comparisons of gas volume fraction and BSD on a horizontal plane for different anode slot heights of (a) 160 mm, (b) 110 mm, (c) 60 mm, and (d) 0 mm.

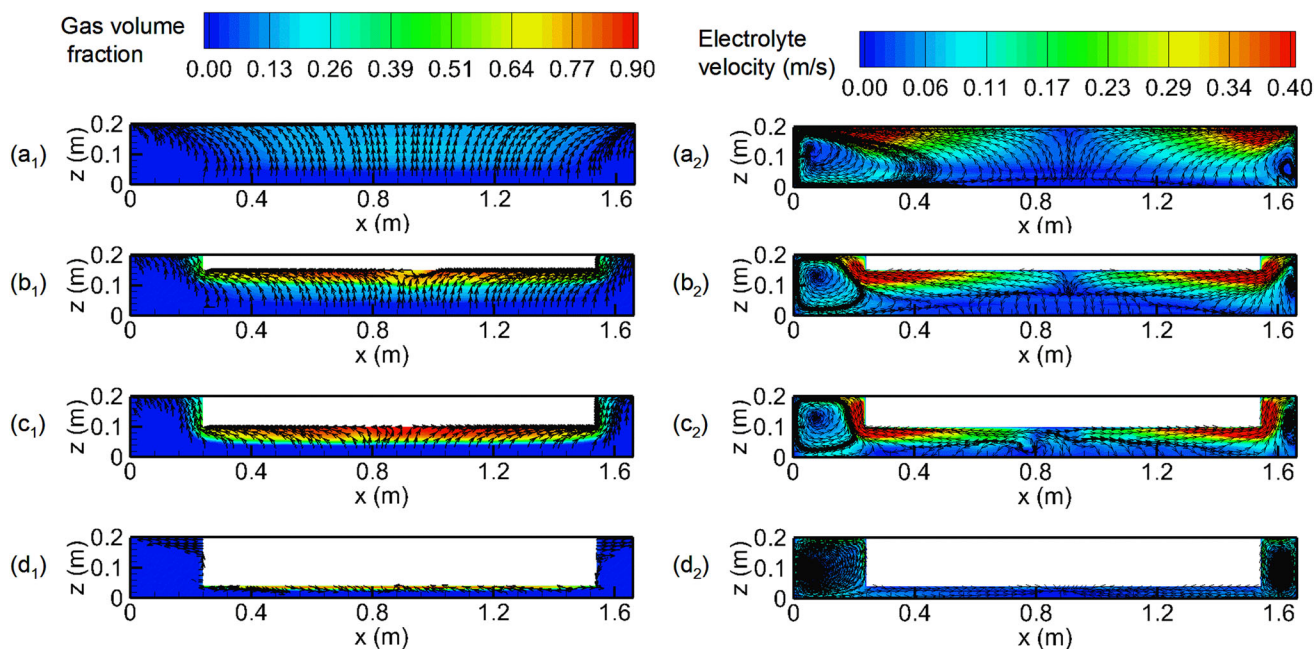


Fig. 6. Predicted distributions of (a<sub>1</sub>–d<sub>1</sub>) gas volume fraction and (a<sub>2</sub>–d<sub>2</sub>) electrolyte velocity on a vertical plane for different anode slot heights.

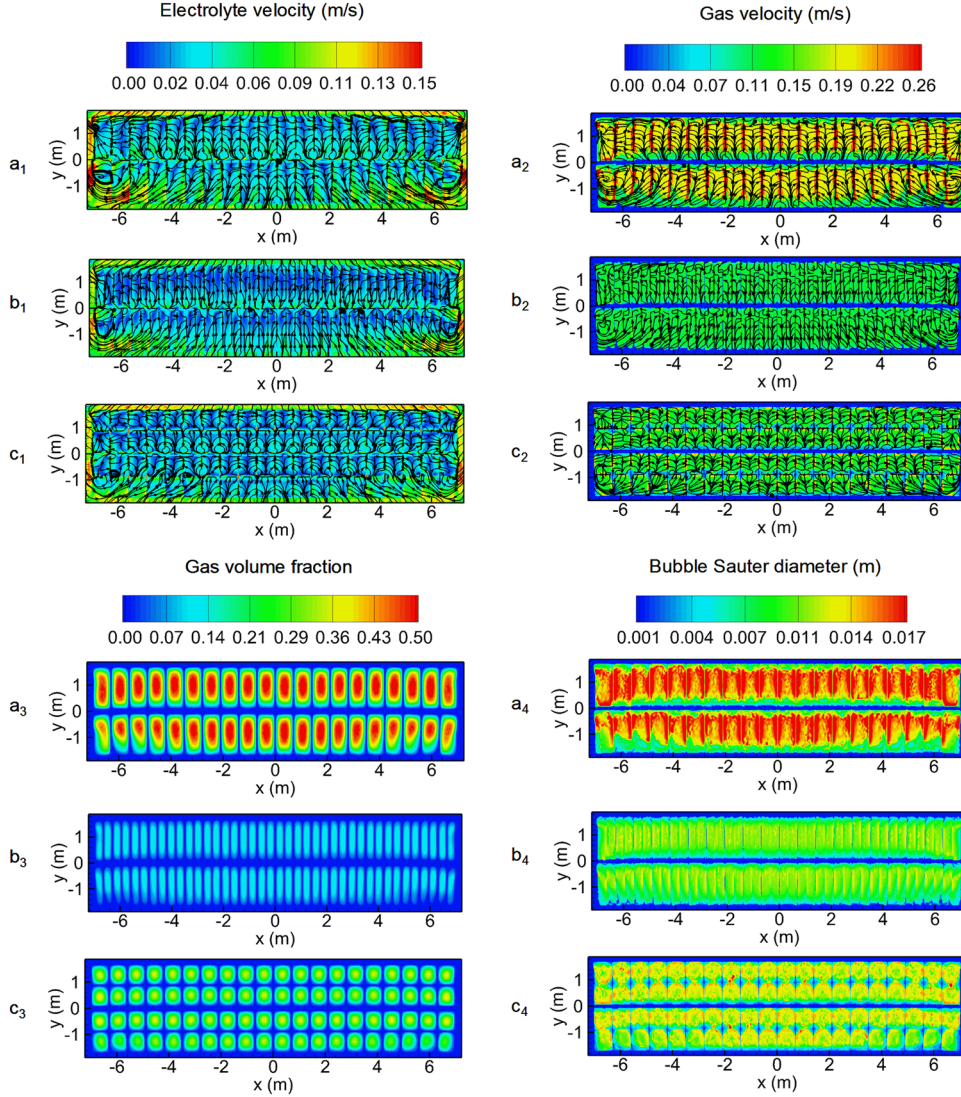


Fig. 7. Comparisons of gas-liquid flow and BSD on a horizontal plane in a 300-kA aluminum electrolysis cell for different anode slot configurations: (a<sub>1</sub>–c<sub>1</sub>) electrolyte velocity, (a<sub>2</sub>–c<sub>2</sub>) gas velocity, (a<sub>3</sub>–c<sub>3</sub>) gas volume fraction, and (a<sub>4</sub>–c<sub>4</sub>) BSD.

slot. The main causes are basically the same as discussed above regarding the results predicted for the different anode slot configurations in the single-anode model, which are not repeated here. Moreover, the results also show that the predicted overall gas volume fractions are apparently influenced by the two large roughly circulatory vortices, especially for the traditional anode. Figure 7a<sub>4</sub>–c<sub>4</sub> shows that the largest bubbles are mainly formed for the traditional anode, less so for the anode with one transversal slot, and least for the anode with one longitudinal slot. Also, the detailed BSD characteristics under the bottom regions of each of the traditional anode and renewed small anode due to the slots are general the same as the results for the single-anode model described above. However, there are also some differences; for example, more smaller bubbles are observed in the upstream regions near the two large, roughly circulatory vortices. This is

mainly because the bubble breakup rate is relatively higher due to the higher electrolyte turbulent energy dissipation rates mainly caused by the EMFs, while the bubble coalescence rate is relatively lower due to the lower gas volume fraction. These observations demonstrate a significant effect of the EMFs on both the gas-liquid flow and bubble dynamic behavior. These results represent a helpful reference to provide new ideas regarding analysis of a more reasonable relationship between the gas bubble behavior and EMFs in further study in this field. Further studies on the gas-liquid two-phase flows in the cell are in progress in our group.

## CONCLUSION

Numerical simulations were carried out to investigate the effects of different anode slot configurations on the gas-liquid multiscale flow

characteristics in aluminum electrolysis cells based on a CFD–PBM coupled model from previous study. The main conclusions can be summarized as follows:

- (1) Both the gas volume fraction and bubble size decrease obviously when transversal or especially longitudinal slots are used. Moreover, the greater the number of both kinds of slot, the smaller the values of these parameters. This is because the gas bubbles can evacuate from longitudinal slots more sufficiently than from transversal slots. The bubble size first decreases then increases gradually along the bubble evacuation direction, with larger bubbles mainly appearing in the upper part of the slot regions. The electrolyte velocity increases remarkably for the anode with one transversal slot.
- (2) The gas volume fraction decreases slightly with increasing anode slot width, mainly because more gas bubbles can effectively evacuate through a larger anode slot width. However, the BSDs are almost the same for the different anode slot widths. One possible reason is that the combined behaviors of bubble coalescence and breakup under the bottom regions of the anode are similar overall.
- (3) With decreasing anode slot height, the gas volume fraction increases, mainly due to the fact that more bubbles can not evacuate vertically from the bottom surface of the anode towards the top surface of the electrolyte effectively. The BSDs show similar features when the anode slot height is decreased from 160 mm to 60 mm, but an entirely different BSD and more larger bubbles can be obtained for the traditional anode.
- (4) The overall electrolyte velocity distributions for the three different anode slot configurations are basically the same, while there also exist some differences in the local flow circulation vortices. Lower gas volume fractions and smaller bubble sizes can be obtained for the slotted anodes than for the traditional anode, especially for the anode with one longitudinal slot. Both the overall gas volume fractions and BSDs are apparently influenced by the two large roughly circulatory vortices caused by the EMFs.

## ACKNOWLEDGEMENTS

The authors are grateful for financial support from the National Natural Science Foundation of China (51704126), Natural Science Foundation of Jiangsu Province (BK20170551, BK20171301), Natural Science Foundation of Higher Education Institutions of Jiangsu Province (17KJB450001), Foundation of Senior Talent of Jiangsu University (2015JDG158), and “Qing Lan” Project Foundation of Jiangsu Province. Our special thanks are due to the anonymous reviewers for insightful suggestions on this work.

## REFERENCES

1. K.E. Einarsrud, I. Eick, W. Bai, Y.Q. Feng, J.S. Hua, and P.J. Witt, *Appl. Math. Model.* 44, 3 (2017).
2. B.J. Moxnes, B.E. Aga, and H. Skaar, *Light Metals 1998*, ed. H. Kvande (San Francisco: TMS, 1998), pp. 247–255.
3. X.W. Wang, *Light Metals 2007*, ed. M. Sørli (Orlando: TMS, 2007), pp. 539–544.
4. K.A. Rye, E. Myrvold, and I. Solberg, *Light Metals 2007*, ed. M. Sørli (Orlando: TMS, 1998), pp. 293–298.
5. K. Vekony and L.I. Kiss, *Metall. Mater. Trans. B* 41, 1006 (2010).
6. M.A. Cooksey and W. Yang, *Light Metals 2006*, ed. T.J. Galloway (San Antonio: TMS, 2006), pp. 359–365.
7. Y.Q. Xue, N.J. Zhou, and S.Z. Bao, *Chin. J. Nonferrous Metals* 16, 1823 (2006).
8. M. Alam, W. Yang, K. Mohanarangam, G. Brooks, and Y.S. Morsi, *Metall. Mater. Trans. B* 44, 1155 (2013).
9. R.G. Aaberg, V. Ranum, and K. Williamson, *Light Metals 1997*, ed. R. Huglen (Orlando: TMS, 1997), pp. 341–346.
10. Z.B. Zhao, Z.W. Wang, B.L. Gao, Y.Q. Feng, Z.N. Shi, and X.W. Hu, *Metall. Mater. Trans. B* 47, 1962 (2016).
11. Y.Q. Feng, M.A. Cooksey, and M.P. Schwarz, *Light Metals 2007*, ed. M. Sørli (Orlando: TMS, 2007), pp. 339–344.
12. J. Li, Y.J. Xu, H.L. Zhang, and Y.Q. Lai, *Int. J. Multiph. Flow* 37, 46 (2011).
13. Y.Q. Feng, M.P. Schwarz, W. Yang, and M.A. Cooksey, *Metall. Mater. Trans. B* 46, 1959 (2015).
14. Q. Wang, B.K. Li, and N.X. Feng, *Metall. Mater. Trans. B* 45, 272 (2014).
15. S.Q. Zhan, Z.T. Wang, J.H. Yang, R.J. Zhao, C.F. Li, J.F. Wang, and J.M. Zhou, *Ind. Eng. Chem. Res.* 56, 8649 (2017).
16. W. Yang and M.A. Cooksey, *Light Metals 2007*, ed. M. Sørli (Orlando: TMS, 2007), pp. 451–456.
17. D.S. Severo, V. Gusberti, E.C.V. Pinto, and R.R. Moura, *Light Metals*, ed. M. Sørli (Orlando: TMS, 2007), pp. 287–292.
18. S. Yang, H.L. Zhang, Y.J. Xu, H.H. Zhang, Z. Zou, J. Li, and Y.Q. Lai, *J. Cent. South Univ. Technol. (Chinese)* 43, 4617 (2012).
19. S.Q. Zhan, M. Li, J.M. Zhou, J.H. Yang, and Y.W. Zhou, *J. Cent. South Univ. Technol.* 22, 2482 (2015).
20. S.Q. Zhan, J.H. Yang, Z.T. Wang, R.J. Zhao, J. Zheng, and J.F. Wang, *JOM* 69, 1589 (2017).
21. S.Q. Zhan, J.F. Wang, Z.T. Wang, and J.H. Yang, *JOM* 70, 229 (2018).